Pis'ma v ZhETF, vol. 93, iss. 4, pp. 217 – 220 © 2011 February 25

Cotunneling effects in GaAs vertical double quantum dots

A. O. Badrutdinov[+*], *S. M. Huang*[*], *K. Kono*[*], *K. Ono*[*], *D. A. Tayurskii*[+1)]

[+] *Institute of Physics, Kazan Federal University, 420008 Kazan, Russia*

[*] *Low Temperature Physics Laboratory, Advanced Science Institute, RIKEN, 351-0198 Wako, Japan*

Submitted 19 November 2010

Resubmitted 11 January 2011

We report observation of Coulomb blockade lifting in GaAs vertical double quantum dot caused by cotunneling processes. One characteristic feature of investigated sample is relatively low potential barriers between dots and reservoirs, which makes cotunneling processes favorable. The measurement of current through the sample under variable bias and gate voltages was carried out at temperature of dilution refrigerator 10 mK. Several distinct features, specific to double dot, were observed and appropriate explanation for them was given.

Semiconductor quantum dots have been a subject of intensive investigation over last two decades. One reason is the proposal [1] to use spin state of electron in a quantum dot as a quantum bit of information (qubit). Another is that quantum dots behave like artificial atoms and follow the rules of atomic physics, including Hund's rule and Pauli exclusion principle [2]. At the moment, plenty of work has been already done, to understand physics of quantum dots and to adopt them for quantum computation [3]. However, the goal seems far away from being reached, still there are a lot of open questions, and the subject attracts a lot of attention.

In the present paper we report investigation of GaAs vertical double quantum dot. Fig.1a shows the schematic view of our sample, and Fig.1c shows the SEM image of a device nominally identical to the investigated one. The device is a sub-micron pillar structure (500 nm diameter) containing two 12 nm thick $In_{0.05}Ga_{0.95}As$ quantum wells, separated by pure GaAs potential barriers. The pillar is surrounded with a gate electrode, which allows tuning the potential in both quantum wells. Quantum wells can exchange electrons with reservoirs made of n-doped GaAs. Applying voltage between source and drain reservoirs leads to current through the double dot.

The class of vertical quantum dot devices, which our sample belongs to, is fabricated from heterostructure of GaAs layers with addition of different impurities. Adding impurity to GaAs leads to the change in bandgap width, and as a result the potential profile of heterostructure has distinct quantum wells and barriers (the one for sample investigated here is shown in Fig.1b). The details of sample fabrication process from original heterostructure are discussed in [5]. We note that most of the double and single vertical dot samples investigated previously [2, 6, 7] had potential barriers made from AlGaAs, with the height of about 200 meV [2]. The specific feature of our sample is that barriers are made from pure GaAs, with relatively low height of about 20 meV. The question we address in this work is how the low height of potential barriers influences the characteristic charge stability diagram of this type of vertical double dot samples.

According to theory of charge transport through a quantum dot (described in details in [3, 8]), the transport is possible only when the electrochemical potential of some charge state of the dot falls in the so called bias window, which is the energy gap between electrochemical potentials of source and drain. Fig.2 shows a plot of (a) current I and (b) differential conductance dI/dV_{SD} of investigated sample, as a function of source-drain voltage V_{SD} and gate voltage V_G, measured at dilution refrigerator temperature of 10 mK and zero magnetic field. It is possible to see clearly the areas of Coulomb blockade (so called Coulomb diamonds), with empty bias window and close to zero current, and nearby areas of second order tunneling, showing relatively weak current, which are specific for double dots, when only one of two dots is involved to charge transport. When the electrochemical potential of certain charge state of double dot enters or leaves the bias window, a step like change of current through the double dot happens, which corresponds to distinct blue lines observed on diagram 2b. The position of these lines provides information about the double dot energy spectrum. Fig.2c shows differential conductance dI/dV_{SD}, as a function of source-drain voltage V_{SD} and gate voltage V_G, for a device, similar by geometry to the investigated one, but having AlGaAs (relatively high) barriers. The charge stability diagram looks essentially similar to diagram 2b, except for less pronounced boundaries between areas of Coulomb blockade and second order tunneling.

[1)] e-mail: dtayursk@gmail.com

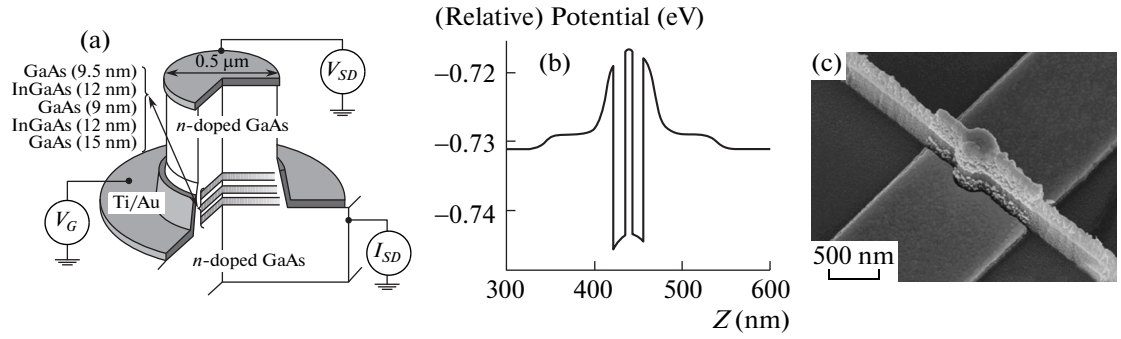

Fig.1. Schematic view of investigated vertical double quantum dot. (a) Dots are defined in $In_{0.05}Ga_{0.95}As$ quantum wells. Potential barriers are formed by pure GaAs layers. (b) Potential profile of original heterostructure conduction band, calculated by Wingreen simulator [4], which is a self-consistent Poisson solver. Z-axis is directed perpendicular to heterostructure surface from the top layer. Small asymmetry relative to center barrier reflects the effect of applied 4 mV source-drain bias, which is the order of voltages applied in experiment. (c) Scanning electron microscope image of a device identical to investigated one

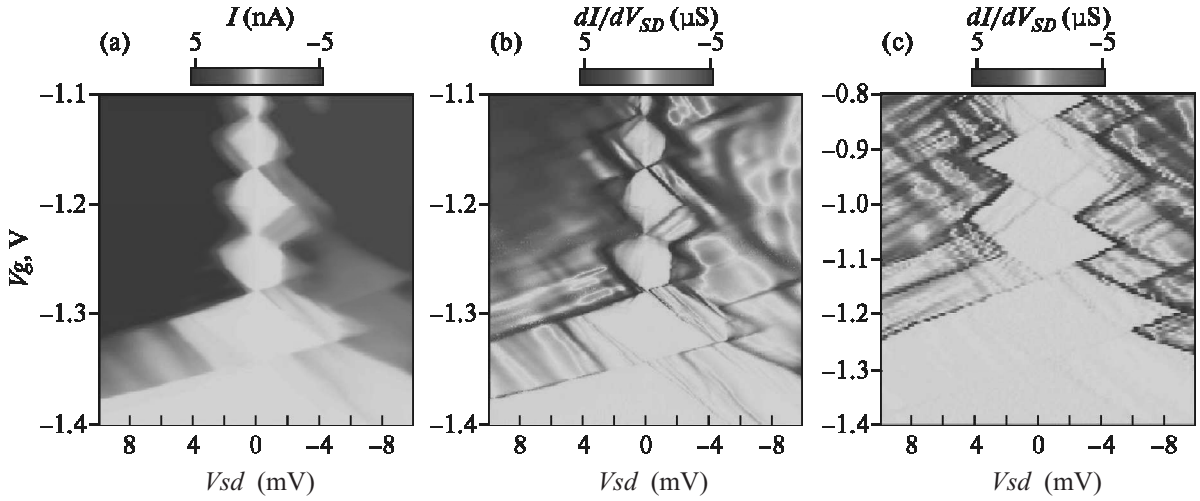

Fig.2. (a) Current I and (b) differential conductance dI/dV_{SD} of investigated low barrier vertical double quantum dot, as a function of source-drain voltage V_{SD} and gate voltage V_G. (c) Differential conductance dI/dV_{SD}, as a function of source-drain voltage V_{SD} and gate voltage V_G, for the vertical double quantum dot analogous to investigated one by geometry, but with relatively high potential barriers made from AlGaAs

Analysis of differential conductance diagram is performed using conventional constant interaction model. The description of this model can be found in [3, 8], here we focus on it's application for analysis. The expressions for electrochemical potentials of two dots can be written for the investigated device as

$$\begin{aligned}\mu_1(N_1,N_2)&=(N_1-\tfrac{1}{2})E_{C1}+N_2E_{Cm}-\alpha_1V_S-\\&-\beta_1V_D-\gamma_1V_G+E_{N1}+\delta,\\ \mu_2(N_1,N_2)&=(N_2-\tfrac{1}{2})E_{C2}+N_1E_{Cm}-\alpha_2V_D-\\&-\beta_2V_S-\gamma_2V_G+E_{N2}.\end{aligned}\qquad(1)$$

Here N_1, N_2 – number of electrons localized in dots 1 and 2, $V_{S(D)}$ – voltage applied to source (drain), V_G – voltage applied to gate, E_C and E_{Cm} – intradot and interdot charging energies, α, β, γ – coefficients of electrostatic coupling between the dot and nearby reservoir, opposite reservoir and gate electrodes correspondingly, E_{Ni} – single-particle energy level of N-th electron in dot i, δ – typical potential offset between two dots. By determination of parameters involved in the above equations, we get all important information about energy spectrum of the double dot. Fig.3a illustrates the analysis. The coefficients can be obtained from the geometry of V-shaped area forming the 1st Coulomb diamond. Within

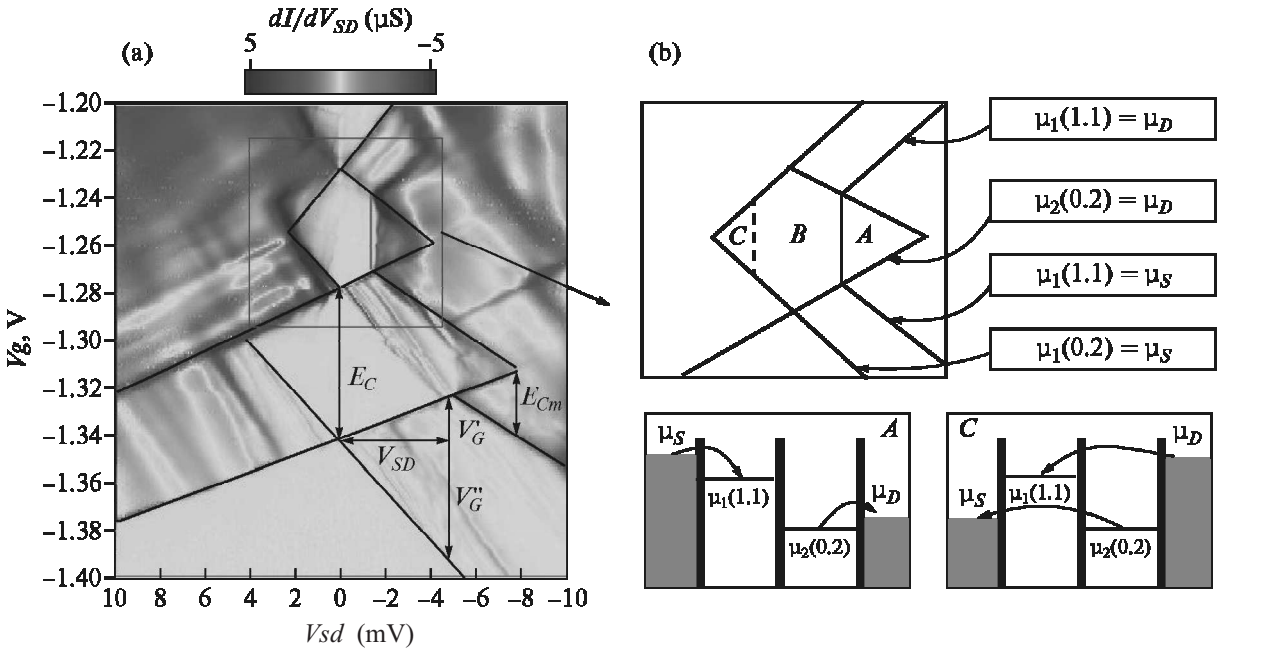

Fig.3. (a) Measured differential conductance dI/dV_{SD}, as a function of V_{SD} and V_G, of the investigated double quantum dot. Black lines on the diagram point out the position of current steps. Parameters E_C and E_{Cm} can be determined explicitly from the diagram. Parameters V_{SD}, V'_G, V''_G are used to determine α, β, γ. (b) Schematic plot of the second Coulomb blockade region where double dot is in (0,2) charge state. Also shown the relative positions of electrochemical potentials, in the areas of A and C of Coulomb diamond, where $\mid \mu_S - \mu_D \mid > \mid \mu_1(1,1) - \mu_2(0,2) \mid$

this area the lowest electrochemical potential of double dot is in bias window. The expressions for α, β, γ in terms of the diagram parameters V_{SD}, V'_G, V''_G is

$$\gamma = \frac{eV_{SD}}{V'_G + V''_G}, \quad \frac{\alpha}{\beta} = \frac{V''_G}{V'_G}, \tag{2}$$

which gives $\alpha = 0.75e$, $\beta = 0.25e$, and $\gamma = 0.07e$, also taking into account that $\alpha + \beta = e$, where e is elementary charge modulus. Another information related to parameters V_{SD}, V'_G, V''_G is the sequence of two dot filling with electrons. If $V''_G > V'_G$, then the next electron will enter dot 2 (which is closer to the drain, in our notation), otherwise, it enters dot 1 (close to the source). So, in case of our sample the first electron resides in dot 2. Looking at consequent V-shape regions forming other Coulomb diamonds, we conclude that the sequence of filling is $(0,1) - (0,2) - (1,2) - (1,3) - (\ldots)$.

Values of E_C and E_{Cm} can be derived explicitly from the charge stability diagram, taking parameters of diagram (in Volts) as shown on Fig.3a, and multiplying them by γ. It gives intradot Coulomb energy $E_C = 4.5$ meV, and interdot Coulomb energy $E_{Cm} = 2$ meV.

One feature we observe on charge stability diagram of investigated sample, which is different from the case of high barrier sample and can not be explained in terms of constant interaction model, is the presence of finite differential conductance areas inside Coulomb diamonds (on the diagram this looks like blue triangles in Coulomb diamond areas). This corresponds to region labeled A in Fig.3b, which is a schematic view of the 2nd Coulomb diamond. We focus on (0,2) charge state, where the corresponding area is most clear, however, other diamonds also show similar features. In that A region the only electrochemical potential within the bias window is $\mu_1(1,1)$, and it can not be involved in charge transport as long as there are two electrons residing in dot 2 (which is exactly the case). However, as soon as source-drain voltage exceeds some certain value, the Coulomb blockade is lifted, and current starts flowing through the double dot. We explain this in terms of cotunneling mechanism, which has been described previously for the case of a single quantum dot [9]. Along the line separating areas A and B on the schematic diagram of Fig.3b, condition $\mu_S - \mu_D = \mu_1(1,1) - \mu_2(0,2)$ is satisfied. In the area, where $\mu_S - \mu_D > \mu_1(1,1) - \mu_2(0,2)$, virtual process of simultaneous tunneling from dot 2 to drain and from source to dot 1, as shown on Fig.3b, is energetically possible. This leads to finite current through the dot, as observed on the charge stability diagram. In area where $\mu_S - \mu_D < \mu_1(1,1) - \mu_2(0,2)$, energy conservation law is not satisfied for this process, and dot is under Coulomb blockade.

One noticeable difference of cotunneling in double dot compared to single dot case is the asymmetry under sign of applied source-drain bias. For (0,2) charge state we see that there is cotunneling area at negative source-drain voltage, but quite usual shape of Coulomb diamond is observed at positive source-drain voltage. In contrast, cotunneling observed in single dot was symmetric under applied voltage sign [9]. This can be explained in the following way. Figure 3b shows the relative position of electrochemical potentials of involved states, in case of double dot under opposite sign of applied bias voltage (area C). In this case each dot forms a potential barrier for electron tunneling from (to) another dot. It makes probability of such transition very low and mechanism becomes totally inefficient. This is not the case for single dot, where the effective barriers are symmetric for cotunneling processes under both signs of applied voltage.

An interesting consequence of a symmetry discussed above is correlation between position of cotunneling area and order of dot filling with electrons. Our double dot is filled in sequence (0,1) (0,2) (1,2) (1,3). In case of the 1st, 2nd and 4th Coulomb diamonds the last electron which enters the dot resides in dot 2, and we observe cotunneling induced current at negative source drain bias. In contrast, in case of 3rd Coulomb diamond last electron resides in dot 1, and relative position of electrochemical potentials necessary for cotunneling happens at positive bias. We also note, that in case of the 1st diamond cotunneling triangle takes place not in the Coulomb blockade area directly, but in the nearby area of second order tunneling. This is the result of initial potential offset between dot 1 and dot 2. In this cotunneling area (0,2) charge state is also in the bias window, so the current results from both cotunneling mechanism involving (1,0) and (0,1) charge states, and from second order tunneling involving (0,2) charge state.

In conclusion, we investigated the charge transport through the vertical double quantum dot with low potential barriers. In particular, we observed lifting of Coulomb blockade, which was explained by manifestation of cotunneling mechanisms, that become favourable with high tunnel rates. For cotunneling in double dot clear asymmetry under applied bias voltage was observed, which is consistent with the difference in effective barrier width, present in case of double dot.

A.O.B. and D.A.T. are supported in part by the Ministry of Education and Science of the Russian Federation (contract # 02.740.11.0797).

1. D. Loss and D. P. DiVincenzo, Phys. Rev. A **57**, 120 (1998)
2. L. P. Kouwenhoven, D. G. Austing, and S. Tarucha, Rep. Prog. Phys. **64**, 701 (2001).
3. R. Hanson, L. P. Kouwenhoven, J. R. Petta et al., Rev. Mod. Phys. **79**, 1217 (2007).
4. K. M. Indlekofer and J. Malindretos, WINGREEN-semiconductor simulator, http://www.fz-juelich.de/isg/mbe/wingreen.html.
5. D. G. Austing, T. Honda, and S. Tarucha, Semicond. Sci. Technol. **11**, 388 (1996).
6. K. Ono, D. G. Austing, Y. Tokura, and S. Tarucha, Science **297**, 1313 (2002).
7. J. Baugh, Y. Kitamura, K. Ono, and S. Tarucha, Phys. Rev. Lett. **99**, 096804 (2007).
8. W. G. van der Wiel, S. De Franceschi, J. M. Elzerman et al., Rev. Mod. Phys. **75**, 1 (2003).
9. S. De Franceschi, S. Sasaki, J. M. Elzerman et al., Phys. Rev. Lett. **86**, 878 (2001).